Using the Diphosphanyl Radical as a Potential Spin Label: Effect of Motion on the EPR Spectrum of an $R^1(R^2)P-PR^1$ Radical

Laurent Cataldo,[a] Cosmina Dutan,[a] Sushil K. Misra,*[b] Sandra Loss,[c] Hansjörg Grützmacher,*[c] and Michel Geoffroy*[a]

Abstract: The EPR spectrum of the novel radical Mes*(CH_3)P–PMes* (Mes* = 2,4,6-(tBu)$_3C_6H_2$) was measured in the temperature range 100–300 K, and was found to be drastically temperature dependent as a result of the large anisotropy of the ^{31}P hyperfine tensors. Below 180 K, a spectrum of the liquid solution is accurately simulated by calculating the spectral modifications due to slow tumbling of the radical. To achieve this simulation, an algorithm was developed by extending the well-known nitroxide slow-motion simulation technique for the coupling of one electron spin to two nuclear spins. An additional dynamic process responsible for the observed line broadening was found to occur between 180 K and room temperature; this broadening is consistent with an exchange between two conformations. The differences between the isotropic ^{31}P couplings associated with the two conformers are shown to be probably due to an internal rotation about the P–P bond.

Keywords: EPR spectroscopy · internal rotation · phosphorus · radicals · spin labeling

Introduction

The spin-labeling technique has been widely used in a large variety of domains, for example, conformation of proteins, fluidity and local order in membranes, and transition phases in various materials.[1] The technique is based on partial averaging of the EPR tensors by molecular reorientation, and allows the exploration of motion over an extremely large range of reorientation. When studying the effect of motion on the properties of a new chemical/biological system, a paramagnetic probe should be chosen such that its g tensor and hyperfine anisotropies conform well to the relevant properties of the system, for example, the viscosity or local order. An examination of the atomic dipolar hyperfine constants reveals that ^{31}P (natural abundance 100%, spin (S) equal to $^1/_2$) provides larger coupling anisotropy than does the unpaired electron in an N–O π^* orbital in the nitroxide radical that is commonly used for spin-labeling experiments. Localization of an unpaired electron in a phosphorus 3p orbital leads, indeed, to a dipolar splitting of 262 G whereas the ^{14}N dipolar coupling associated with an electron totally confined in a nitrogen 2p orbital is only 40 G.[2] The main problem in using phosphorus radicals as spin labels is their enhanced reactivity. As a consequence, these compounds are not stable and rapidly disappear in solution. During the last decade, considerable progress has been made in the chemistry of low-coordinated phosphorus compounds in that numerous stable diamagnetic molecules containing a nonsaturated P=C or P=N bond have been synthesized.[3] In this context, further progress was accomplished recently with the synthesis of a phosphorus analogue of hydrazyl in our laboratory.[4] This di-

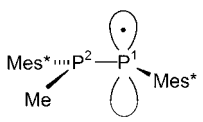

1

[a] Dr. L. Cataldo, Dr. C. Dutan, Prof. M. Geoffroy
Department of Physical Chemistry, 30 quai Ernest Ansermet
University of Geneva, 1211 Geneva 4 (Switzerland)
Fax: (+41) 22-379-6552
E-mail: michel.geoffroy @chiphy.unige.ch

[b] Prof. S. K. Misra
Department of Physics, Concordia University
Montreal, Quebec H3G 1M8 (Canada)
Fax: (+1) 514-848-2828
E-mail: skmisra@vax2.concordia.ca

[c] Dr. S. Loss, Prof. H. Grützmacher
Department of Chemistry and Applied Biosciences
ETH-Hönggerberg, 8093 Zürich (Switzerland)
Fax: (+41) 1-633-1032
E-mail: gruetzmacher@inorg.chem.ethz.ch

Supporting information for this article is available on the WWW under http://www.chemeurj.org/ or from the author.

 DOI: 10.1002/chem.200401276

phosphanyl radical (**1**) was found to be stable in solution due to the presence of the sterically demanding aryl group 2,4,6-tri(*tert*-butyl)benzene, Mes*, which protects the dicoordinated phosphorus atom efficiently. Therefore, it is possible to study experimentally the effect of molecular tumbling on the EPR spectra of a radical whose electron is delocalized in a phosphorus–phosphorus π orbital. Exploiting this approach, a study of EPR spectra of **1** at various temperatures is reported in the present work. The temperature dependence of the spectrum was analyzed by simulating the EPR signals as a function of the diffusion constant. No simulation program for slow tumbling is available to date for a system involving coupling of an electron spin with two nuclei, although an algorithm is available to simulate spectra for reorientation of radicals coupled with one nucleus, as developed by Schneider and Freed for nitroxides,[5] wherein one electron spin ($S=^1/_2$) is coupled to one nucleus of arbitrary spin value. Therefore, a major part of the present study has been devoted to extending the nitroxide algorithm to accommodate the case of one electron spin coupled to two nuclei of arbitrary spin value. The details of this extension are outlined in the slow-tumbling section (see Results).

Experimental Section

The synthesis of radical **1** was performed by reduction of the phosphonium salt [Mes*(Me)P=PMes*]CSO_3F_3 with tetrakis(dimethylamino)ethylene as described in ref. [4]. The resulting yellow-orange crystals were dissolved in THF. The solution was then degassed by several freeze-pump-thaw cycles. EPR spectra were recorded on a Bruker 200 spectrometer (9 GHz, 100 kHz field modulation) equipped with a ER-4111 variable-temperature attachment.

The *g* and hyperfine tensors of **1** were determined from single-crystal EPR measurements. The sample used was a diphosphane Mes*(Me)P–P(Me)Mes* crystal, grown in the presence of **1**.

The slow-motion spectra were simulated by using an extension of the program by Schneider and Freed (SF hereafter) previously written for nitroxide spin labels.[5] Following the SF procedure, one uses the parameter input program LBLL, followed by the program EPRLL for spectral calculation. The spectrum is finally calculated by the program TDLL, which processes the Lanczos tridiagonal matrix generated by EPRLL.[6,7] (The details are the same as those described in the SF procedure, to which reference should be made.) The simulations were carried out on a PC and visualized with the Microcal Origin 6.0 software.

Results

EPR tensors: For each orientation of the doped single crystal of diphosphane with respect to the direction of the external magnetic field, the spectrum was observed to be composed of two subspectra (A and B), each exhibiting a hyperfine interaction with two nuclei of spin $^1/_2$, consistent with the presence of the R(R′)P–PR′ species. Analysis of the angular variation of the spectra in three perpendicular planes related to the morphology of the diphosphane crystal, led to two sets of tensors (set {A} and set {B}). The eigenvalues calculated for set {A} are practically equal to those of set {B} and are reported in Table 1. They indicate that, in the diphosphane crystal, radical **1** occupies two magnetically inequivalent orientations dictated by the symmetry of the host crystal.

Table 1. Principal values[a] of the EPR tensors for **1** trapped in a single crystal of diphosphane.

g tensor	$^{31}P^1$ coupling tensor [gauss]	$^{31}P^2$ coupling tensor [gauss]
2.0022 ± 0.0002	1.8 ± 2.4	116.4 ± 1.9
2.0062 ± 0.0002	12.8 ± 1.7	122.3 ± 0.3
2.0155 ± 0.0002	252.8 ± 1.8	180.1 ± 1.1

[a] The differences in the values obtained for sets {A} and {B} are indicated by ±.

From Table 1, the average value for *g* is found to be 2.0079. The hyperfine interactions consist of Fermi contact and dipolar coupling. By assuming that all eigenvalues of the hyperfine tensor are positive, the following are estimated to be its various components: isotropic coupling constants $A_{iso}(P^1)=89.1$ and $A_{iso}(P^2)=139.6$ G; anisotropic coupling constants $\tau_x=-87.3$, $\tau_y=-76.3$, and $\tau_z=163.6$ G for P^1 and $\tau_i=-23.2$, $\tau_j=-17.3$, and $\tau_k=40.5$ G for P^2 (P^1 = dicoordinate phosphorus, P^2 = tricoordinate phosphorus).

EPR spectra were simulated at various temperatures (vide infra) by using the EPR tensors obtained for site A in the experimental reference frame, as listed in Table 2.

Table 2. EPR tensors for **1** (site A, experimental reference frame).

g tensor	$^{31}P^2$ hyperfine tensor [gauss]	$^{31}P^1$ hyperfine tensor [gauss]
2.0157, 0.0000, −0.0006	121.65, 2.78, 0.37	10.06, 26.50, −7.04
−0.0000, 2.0024, 0.0012	2.78, 161.39, −30.33	26.50, 243.60, −31.91
−0.0060, 0.0012, 2.0061	0.37, −30.33, 134.89	−7.04, −31.91, 12.69

Temperature dependence of EPR spectra: As shown in Figure 1, the EPR spectra obtained for a solution of **1** in THF are strongly temperature dependent between 100 and 300 K. In this range, all modifications to the spectrum are reversible. However, **1** decomposes when it is kept above room temperature for extended periods of time.

Simulation of EPR spectra recorded at various temperatures

Slow tumbling: The slow-motion spectra simulated in this paper are based on the theory described by Freed,[8] and were calculated by using an extension of the algorithm developed by Schneider and Freed to treat the case of a radical characterized by an electron spin of $^1/_2$ coupled to a nucleus with an arbitrary spin value (*I*).[5]

Briefly, the algorithm solves the stochastic Liouville equation to calculate the time evolution of the relevant density matrix from which the unsaturated, high-field, frequency-swept spectrum can be calculated, as shown in Equation (1):

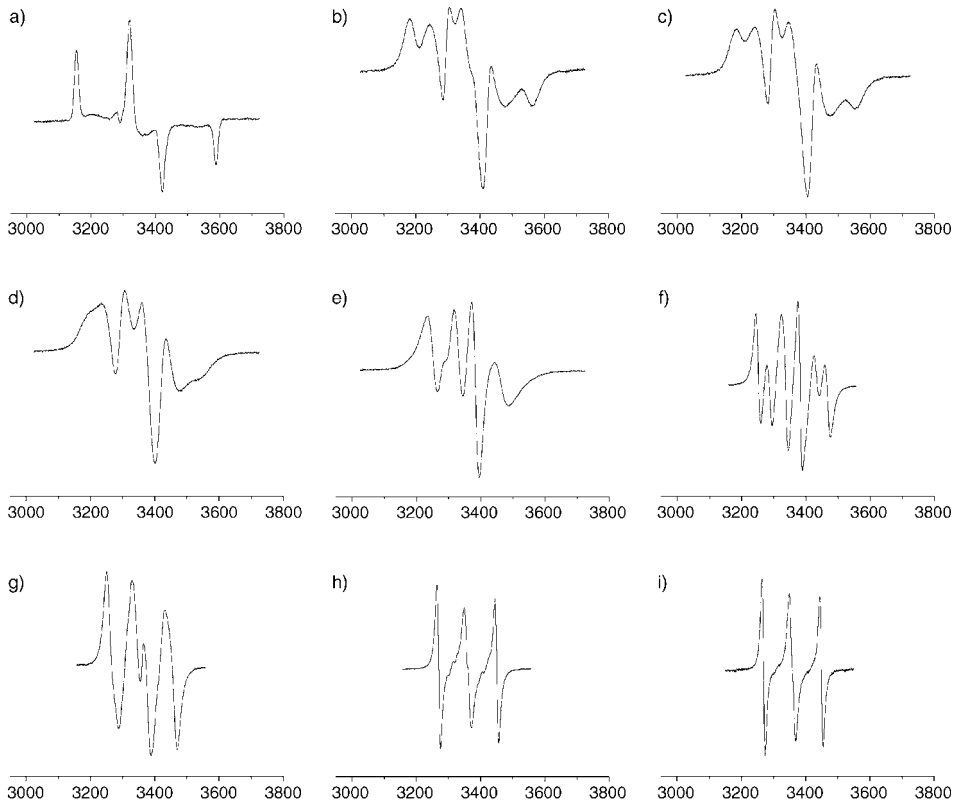

Figure 1. Experimental EPR spectra (all the axes represent the intensity of the magnetic field in gauss) obtained with a solution of radical **1** in THF at various temperatures: spectra a)–i) correspond to 100, 160, 165, 170, 180, 220, 245, 275, and 300 K, respectively.

$$I(\omega-\omega_0) = \left(\frac{1}{\pi}\right)\langle\langle \nu|[(\tilde{\Gamma}-iL) + i(\omega-\omega_0)\mathfrak{l}]^{-1}|\nu\rangle\rangle \qquad (1)$$

in which ω is the sweep frequency ($\omega_0 = g_0\mu_B B_0/\hbar$), where B_0 is the intensity of the external magnetic field, $g_0 = (g_{xx}+g_{yy}+g_{yy})/3$, μ_B is the Bohr magneton, and $\hbar$ is the Planck constant divided by 2π; L is the Liouville superoperator (LSO) associated with the orientation-dependent spin Hamiltonian; $\tilde{\Gamma}$ is the "symmetrized" diffusion operator used to model the classical reorientational motion; i is the imaginary number; and $\mathfrak{l}$ is the identity operator. In addition, $|\nu\rangle$ is the starting vector, which includes both the electron and nuclear spin operators for the allowed EPR transitions and the equilibrium probability distribution function for the orientation of the radicals.

The most significant steps that we made in the extension of this algorithm are as follows.

Inclusion of the hyperfine interaction with the second nucleus, and its Zeeman interaction: The values of the hyperfine-tensor components for the two nuclei, as determined here in our laboratory, were entered to be used in the subroutine MATRLL in the source code for calculation of the relevant matrix elements. No transformations from the principal axes systems were therefore made to the director frame (space fixed) and then to the diffusion frame (body fixed). For an arbitrary orientation, as is the case here, all five irreducible spherical tensor operators of second order are required. However, those of the order (2, ±1), also required here, are not listed in SF and were therefore added.

Extension of the starting vector to include two nuclear spins and their projections while maintaining the time-reversal invariance: In the high-field approximation and slow motional limits, as described in SF, the starting vector was extended to have the following form, shown in Equation (2):

$$\begin{aligned}&|LMK';1,0;p_1^I,q_1^I;p_2^I,q_2^I\gg\\ &= [2(1+\delta_{k,0}\delta_{p_1^I,0}\delta_{p_2^I,0})]^{-1/2}\\ &\times(|LMK';1,0;p_1^I,q_1^I;p_2^I,q_2^I\gg\\ &+(-1)^{L+M}|L-MK';1,0;\\ &-p_1^I,q_1^I;-p_2{}^I,q_2{}^I\gg)\end{aligned} \qquad (2)$$

in which, $p^I = M_I - M_I'$ and $q^I = M_I + M_I'$, where M_I and M_I' are the nuclear magnetic quantum numbers in the two states involved in the EPR transition and the integers L, M, and K characterize the Wigner rotation functions. (The numbers 1,0 stand for quantities corresponding to p^I,q^I for the electron spin.) In writing this equation, the symmetry of the matrix elements of the LSO under the simultaneous reversal of the signs of the electronic magnetic quantum number (M) and those of the p_1^I,p_2^I indices for the two nuclei, has been taken into account to preserve the time-reversal invariance.

The two most important parameters are the parallel (d_{zz}) and perpendicular (d_{xy}) components of the rotational diffusion tensor. The parallel component is related to the correlation time for the motion of the spin probe about the symmetry axis of the diffusion tensor, whereas the perpendicular component is related to the motion perpendicular to the symmetry axis. In an isotropic situation the two components become equal to each other (d).

Simulation of exchange-broadened spectra: The program required for this part of the simulation uses the general lineshape equation for intramolecular exchange between two sites, as reported by Heinzer.[9] The EPR spectrum is calculated in the Liouville space by summing the elements of the ρ^{-+} vector (ρ = density matrix). In addition to the transition values, the program takes into account the populations of the two conformers, the intrinsic relaxation terms T_2^{-1}, and the rate constants k_{ij}.

Comparison of simulated spectra with experimental spectra: As seen from Figure 2, the EPR tensors determined from single-crystal experiments lead to a very satisfactory simulation of the frozen-solution spectrum.[10]

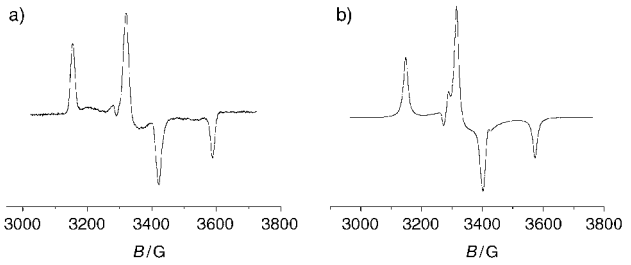

Figure 2. a) Frozen-solution spectrum recorded at 100 K. b) Spectrum simulated with the EPR tensors given in Table 2.

Between 100 and 150 K the experimental spectrum is almost unaffected by temperature. In the temperature range 150–160 K, close to the melting point of the sample, the spectrum exhibits some modifications but as several phases probably coexist in the sample, the resulting spectrum is hard to simulate. At 160 K, the experimental spectrum (Figure 1) is composed of seven lines, which are approximately reproduced in the spectrum simulated with the program described in the slow-tumbling section (see Results). Above 165 K, the sample is likely to be homogeneous and its viscosity allows the irregularly shaped radical to tumble freely. As shown in Figure 1 at 170 K, the spectrum is composed of a triplet of doublets. A good simulation of this pattern can be obtained by assuming an isotropic reorientation of the radical with a diffusion rate, d, equal to $0.175\times10^9\ s^{-1}$ (Figure 3). Increasing the temperature causes the external doublets to coalesce progressively. The simulation of the spectrum representing this process is performed by increasing the diffusion constant (e.g., $d=0.2\times10^9\ s^{-1}$ for the spectrum recorded at 175 K, Figure 3). For a d value of $0.3\times10^9\ s^{-1}$, four lines are present in the simulated spectrum in good agreement with the spectrum recorded at 180 K. However, whereas additional increases in d cause only a narrowing of the line width of the four signals, several drastic modifications affect the experimental spectrum between 185 and 300 K. It is worth noting that the two ^{31}P isotropic coupling constants estimated from the room-temperature data do not correspond to the average value calculated from the single-crystal hyperfine tensors with the values $A_{iso}(P^2)=88$ and $A_{iso}(P^1)=139$ G. Furthermore, the broadening of the central signal is not consistent with the hyperfine structure due to the presence of two equivalent ^{31}P nuclei.

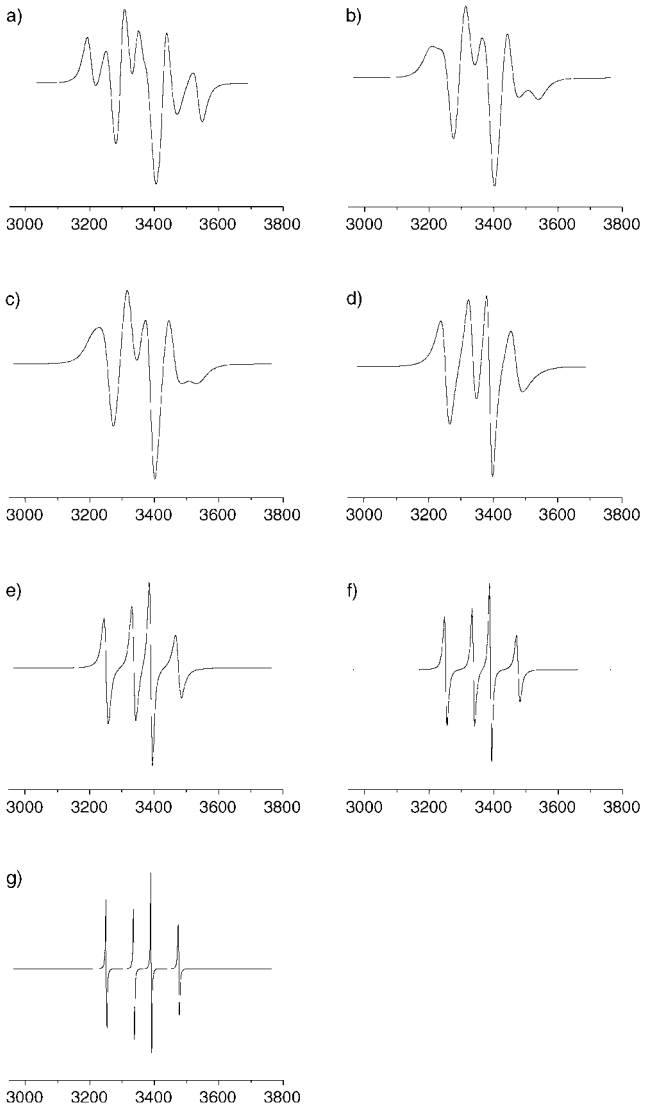

Figure 3. Simulation of the slow-tumbling spectra (all the axes represent the magnetic flux density in gauss) as a function of the diffusion constant. Spectra a)–g) correspond to $d=0.1\times10^9$ (160 K), 0.175×10^9 (170 K), 0.2×10^9 (175 K), 0.3×10^9 (180 K), 0.6×10^9, 1.0×10^9, and $5.0\times10^9\ s^{-1}$, respectively.

Discussion

The tensors determined from the single-crystal measurements agree with those of the frozen-solution spectrum. Using them, a good simulation of the spectra observed between 160 and 180 K is obtained. The variations in the EPR spectra of **1** clearly illustrate the dependence of the spectra on tumbling for a diffusion rate varying between 0.1×10^9 and $0.3\times10^9\ s^{-1}$. These variations do not only affect the line width of the signals but also the number of EPR lines. They confirm that, in this range, the sensitivity to the motion of the phosphorus-containing radical is considerably larger than that for a nitroxide radical (see Supporting Information).

Increasing the diffusion rate to above $0.3\times10^9\ s^{-1}$ does not change the number and positions of the lines, it only causes a decrease in their line widths. However, additional transitions appear in the experimental spectrum above 180 K. Between 200 and 220 K, six lines are clearly detected. Above 245 K, the two low-field lines, as well as the two

high-field lines, coalesce with each other. At higher temperatures, the two central lines begin to merge. The observation that the slow-tumbling simulation cannot reproduce the experimental temperature dependence of the spectrum above 185 K reveals that an additional dynamic phenomenon is present above this temperature. The associated spectral modifications are likely to be due to an exchange between two conformations. They suggest that, above 185 K, **1** can adopt a second conformation of slightly higher energy. The effect of this dynamic process on the spectrum can be calculated by using the simulation program mentioned in the section on simulation of exchange-broadened spectra (see Results). Each conformation is characterized by its own isotropic coupling constants and populations. The isotropic constants of the lower energy structure (conformation C1) are those determined by the single-crystal measurements: $A_{iso}(P^1)=88$, $A_{iso}(P^2)=139$ G. The coupling constants of the second conformation (C2) were determined by fitting the simulated spectra to the experimental spectra. As shown in Figure 4, a satisfactory simulation was achieved by using the following constants for the second conformation: $A_{iso}(P^1)=110$ and $A_{iso}(P^2)=50$ G, and by adjusting the exchange rate constant (k) for the spectra recorded at 200, 225, 245, and 300 K.

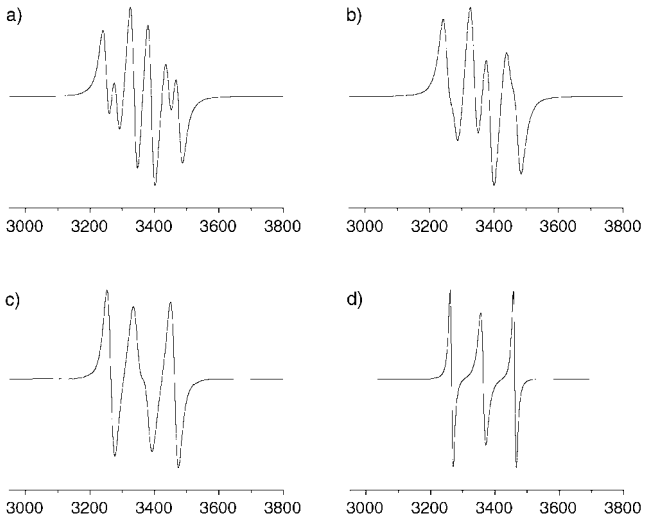

Figure 4. Simulation of the spectra (all the axes represent the intensity of the magnetic field in gauss) resulting from exchange between conformations C1 and C2 as a function of the rate constant. Spectra a)–d) correspond to $k=0.176\times10^8$ (220 K), 1.06×10^8 (245 K), 2.64×10^8 (275 K), and 7.92×10^8 s^{-1} (300 K), respectively.

These values can be attributed to a temperature-dependent internal rotation about the P–P bond. At low temperatures, below 185 K, the dihedral angle (ζ) between the spin-carrying p π orbital of the dicoordinated phosphorus (P^1) and the lone-pair containing orbital of the pyramidal, tricoordinated phosphorus (P^2), as shown in Figure 5, is small and leads to conjugation between these two atoms. The rather large A_{iso} value for P^2 reflects the non-negligible s character of this latter orbital ($\rho_s=139/4752=0.029$,[11] $\rho_p=0.15$). At temperatures above 185 K, a second conformation of **1** appears with a larger dihedral angle between the p π orbital (P^1) and the sp^n orbital (P^2). The resulting decrease in conjugation causes a decrease in the P^2 spin density ($\rho_s=50/4857=0.010$) while the increase in the spin localization on P^1 leads to an increase of the isotropic coupling constant through an internal spin polarization mechanism ($A_{iso}(P^1)$ passes from 88 to 110 G). The existence of this second conformation is probably associated with the presence of the cumbersome Mes* substituents, which are expected to give rise to strong sterical interactions. The activation energy E_a for the exchange between conformations C1 and C2 can be estimated from an Arrhenius plot (see Supporting Information); E_a is found to be close to 6 kcal mol^{-1}, a value which is slightly higher than that measured for the rotation barrier of the ·PH group around the C–P bond in the phosphinyl radical Tript-·PH (Tript = triptycene).[12]

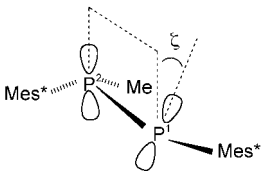

Figure 5. Definition of the dihedral angle ζ [°].

Conclusion

The study presented here shows that the EPR spectrum of the diphosphanyl radical (**1**) is very sensitive to its rotational reorientation, as a result of the large anisotropy of the ^{31}P coupling tensors. This radical can therefore be potentially used as a spin label as drastic modifications of the spectrum occur when the diffusion parameter varies between 0.1×10^9 and 0.6×10^9 s^{-1}. This favorable property is, however, complicated by the temperature dependence of the internal rotation around the P–P bond on the signal pattern. An important conclusion from the findings in this work is that not only the stability of phosphorus-centred radicals like **1** has to be enhanced, they also have to be sufficiently rigid to make them applicable as spin labels. Further investigations are in progress in our laboratory to achieve these goals.

Acknowledgements

Financial support of this work by the Swiss National Science Foundation is gratefully acknowledged. S.K.M. is grateful to Professor Jack Freed of Cornell University for providing him with the opportunity to spend a part of his sabbatical leave in his laboratory when the extension of the slow-motion technique to the hyperfine coupling with two nuclei was made.

[1] *Spin Labeling, Theory and Applications* (Ed.: L. J. Berliner), Academic Press, New York **1976**.
[2] Atomic anisotropic coupling constants obtained from Hartree–Fock calculations: J. R. Morton, K. F. Preston, *J. Magn. Reson.* **1978**, *30*, 577.

[3] a) K. B. Dillon, F. Mathey, J. F. Nixon, *Phosphorus: The Carbon Copy*, Wiley, New York, **1998**; b) *Multiple Bonds and Low Coordination in Phosphorus Chemistry* (Eds.: M. Regitz, O. Scherrer), Thieme, Stuttgart, **1999**; c) *Phosphorus-Carbon Heterocyclic Chemistry: The Rise of a New Domain* (Ed.: F. Mathey), Pergamon, Amsterdam, **2001**.
[4] S. Loss, A. Magistrato, L. Cataldo, S. Hoffmann, M. Geoffroy, U. Röthlischberger, H. Grützmacher. *Angew. Chem.* **2001**, *113*, 749; *Angew. Chem. Int. Ed.* **2001**, *40*, 723.
[5] D. J. Schneider, J. H. Freed in *Biological Magnetic Resonance*, *Vol. 8* (Eds.: L. J. Berliner, J. Reuben), Plenum, New York, **1989**, pp. 1–75.
[6] C. Lanczos, *J. Res. Natl. Bur. Stand.* **1950**, *45*, 255.
[7] a) G. Moro, J. H. Freed, *J. Phys. Chem.* **1980**, *84*, 2837; b) G. Moro, J. Freed, *J. Chem. Phys.* **1981**, *74*, 3757.
[8] J. H. Freed in *Spin Labeling*, *Theory and Applications* (Ed.: L. J. Berliner), Academic Press, New York, **1976**, Chapter 3.
[9] J. Heinzer, *Mol. Phys.* **1971**, *22*, 167.
[10] Simulation with the WINEPR SimFonia program (Bruker). The tensors were expressed in the reference frame that diagonalizes the *g* tensor.
[11] As reported by Morton and Preston (see ref. [2]), the atomic isotropic coupling constant for ^{31}P is assumed to be equal to 4752 G. The atomic anisotropic coupling $2B_0 = 262$ G.
[12] a) G. Ramakrishnan, A. Jouaiti, M. Geoffroy, G. Bernardinelli, *J. Phys. Chem.* **1996**, *100*, 10861; b) M. Brynda, T. Berclaz, M. Geoffroy, G. Ramakrishnan, *J. Phys. Chem. A* **1998**, *102*, 8245.

Received: December 10, 2004
Published online: April 8, 2005